



HAL
open science

How a dc Electric Field Drives Mott Insulators Out of Equilibrium

Pascale Diener, Etienne Janod, B. Corraze, M. Querre, C. Adda, Maryline Guilloux-Viry, Stéphane Cordier, A. Camjayi, M. Rozenberg, M. p. Besland, et al.

► **To cite this version:**

Pascale Diener, Etienne Janod, B. Corraze, M. Querre, C. Adda, et al.. How a dc Electric Field Drives Mott Insulators Out of Equilibrium. *Physical Review Letters*, 2018, 121 (1), 10.1103/PhysRevLett.121.016601 . hal-01848488

HAL Id: hal-01848488

<https://hal.science/hal-01848488>

Submitted on 18 Jan 2024

HAL is a multi-disciplinary open access archive for the deposit and dissemination of scientific research documents, whether they are published or not. The documents may come from teaching and research institutions in France or abroad, or from public or private research centers.

L'archive ouverte pluridisciplinaire **HAL**, est destinée au dépôt et à la diffusion de documents scientifiques de niveau recherche, publiés ou non, émanant des établissements d'enseignement et de recherche français ou étrangers, des laboratoires publics ou privés.

How a dc Electric Field Drives Mott Insulators Out of Equilibrium

P. Diener,^{1,*} E. Janod,¹ B. Corraze,¹ M. Querré,^{1,2} C. Adda,¹ M. Guilloux-Viry,² S. Cordier,²
A. Camjayi,³ M. Rozenberg,⁴ M. P. Besland,¹ and L. Cario^{1,†}

¹*Institut des Matériaux Jean Rouxel, Université de Nantes, CNRS, 2 rue de la Houssinière, BP32229, 44322 Nantes Cedex 3, France*

²*Univ Rennes, CNRS, ISCR (Institut des Sciences chimiques de Rennes) UMR 6226, 35000 Rennes, France*

³*Departamento de Física, FCEyN, Universidad de Buenos Aires and IFIBA, Pabellón I, Ciudad Universitaria, 1428 CABA, Argentina*

⁴*Laboratoire de Physique des Solides, Université Paris Sud, 91405 Orsay Cedex, France*



(Received 7 March 2017; published 3 July 2018)

Out of equilibrium phenomena are a major issue of modern physics. In particular, correlated materials such as Mott insulators experience fascinating long-lived exotic states under a strong electric field. Yet, the origin of their destabilization by the electric field is not elucidated. Here we present a comprehensive study of the electrical response of canonical Mott insulators GaM_4Q_8 ($M = \text{V, Nb, Ta, Mo}$; $\text{Q} = \text{S, Se}$) in the context of a microscopic theory of electrical breakdown where in-gap states allow for a description in terms of a two-temperature model. Our results show how the nonlinearities and the resistive transition originate from a massive creation of hot electrons under an electric field. These results give new insights for the control of the long-lived states reached under an electric field in these systems which has recently open the way to new functionalities used in neuromorphic applications.

DOI: [10.1103/PhysRevLett.121.016601](https://doi.org/10.1103/PhysRevLett.121.016601)

The study of correlated electronic systems in nonequilibrium conditions is rapidly expanding. These systems have already fascinating properties at equilibrium such as high-temperature superconductivity or colossal magnetoresistance. The recent advances of ultrafast pump-probe techniques and cold atom physics have highlighted the enormous potential of driving such systems out of equilibrium. It is a novel powerful way to discover unusual electronic states which are absent at equilibrium, the so-called hidden phases [1]. In Mott insulators, for instance, two recent discoveries, namely, the stabilization of a hidden quantum state in TaS_2 by a single-shot ultrafast laser pulse [2] and light-induced superconductivity in a stripe-ordered cuprate [3], illustrate the relevance of this approach. In Mott insulators, both ultrafast single-photon absorption ($h\nu > \text{Mott-Hubbard gap } \Delta_{\text{MH}}$) [4] and terahertz excitation ($h\nu < \Delta_{\text{MH}}$) [5] yield a transient Mott insulator to metal transition related to a massive creation of hot carriers.

An alternative way to bring an insulating system out of equilibrium is the application of a strong dc electric field, beyond the polarization regime [6]. A classical example is dielectric breakdown in semiconductors [7]. However, the effect of strong dc electric fields on correlated systems is much more complex. Recent results obtained on canonical Mott insulators are remarkable, with the realization, above a threshold electric field, of long-lived metallic states with low-temperature granular superconductivity [8]. However, despite numerous theoretical studies [9–16], the mechanism at the origin of the system destabilization under an electric field is still under debate. Models invoking the Landau-Zener tunneling effect (see, e.g., Refs. [9,17], and references

therein) capture neither the correct order of magnitude for the threshold electric field nor its strongly temperature-dependent behavior [18]. Theoretical approaches proposed more recently may avoid these issues but at the cost of a limited range of validity. In fact, they require one to tune the Mott insulators inside [13] or within an extremely narrow window close to the coexistence domain between the correlated metal and Mott insulating states [15]. Thus, the models proposed so far can hardly explain the insulator to metal transitions induced by moderate electric fields, which appear quite universally in narrow and large gap Mott insulators. In that context, it was recently noted in a review by Aoki *et al.* [6] that it is “an interesting challenge to develop a microscopic understanding of the nonlinear transport properties of correlated systems from a universal viewpoint.” Here we show that a microscopic theory based on the description proposed by Fröhlich in the 1940s for the dielectric breakdown in imperfect semiconductors can be successfully applied for Mott insulators. As predicted by this model, we observed that the canonical Mott insulators GaM_4Q_8 ($M = \text{V, Nb, Ta, Mo}$; $\text{Q} = \text{S, Se}$) exhibit (i) nonlinear electrical properties at a low field that results from an elevation of their electronic temperature and (ii) electrical breakdown above a threshold field when nonequilibrium conditions (called hereafter “out of equilibrium”) are reached and lead to a divergence of the electronic temperature.

The foundations of current theories of intrinsic electrical breakdown in band semiconductors were laid more than 70 years ago by Fröhlich and Seitz [7,19–22]. In particular, Fröhlich studied the effect of trapped electrons on the electrical response [19]. He shows that, if their density is

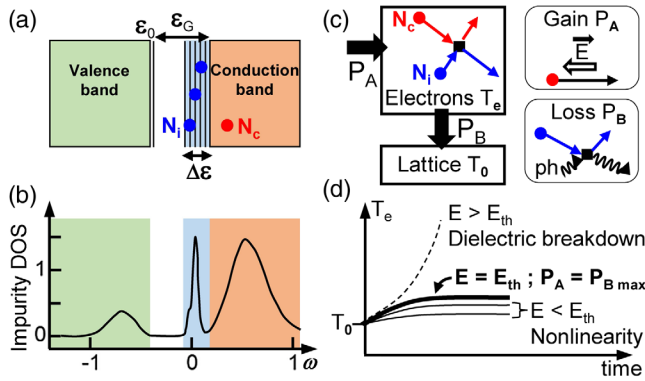


FIG. 1. Schematic description of the breakdown in the dirty limit. (a) The density of states presents a gap ε_G between the fundamental impurity level ε_0 and the conduction band (red region), with discrete impurity levels spread on the energy width $\Delta\varepsilon$ (blue region). Some electrons in the impurity levels (N_i) and in the conduction band (N_c) are indicated by the blue and red points. (b) Simulation of the density of states of the Mott insulator GaTa_4Se_8 at finite temperature $T = 116$ K. An in-gap peak (blue region) is present at the edge of the upper Hubbard band (red region) due to the weak electronic doping ($n = 1.045$). (c) Thermal balance of the electronic system. Electrons have a temperature T_e distinct from the lattice temperature T_0 . P_A and P_B are the heating and cooling powers, respectively, sustained by the electrons. (d) Time evolution of the electronic temperature under several values of the electric field.

sufficient, a specific breakdown mechanism appears, hereafter called the dielectric breakdown in the dirty limit. The starting ingredient of the theory is the specific density of states (DOS) described Fig. 1(a). The trapped electrons have a ground state ε_0 located at ε_G below the conduction band and several localized excited energy levels distributed on a typical energy width $\Delta\varepsilon$ and located just below the conduction band. Unlike the electrons in the conduction band, the trapped electrons cannot be accelerated by an electric field, because these levels are not continuously distributed. However, if their density is high enough, they give rise to an efficient scattering with the conduction electrons. They act as a reservoir for the electronic energy gained by the conduction electrons and have a central role in the stability of the electronic system.

The DOS assumed in Fröhlich's model and represented in Fig. 1(a) is actually particularly relevant for Mott insulators in the presence of weak doping. Theoretically, doping in correlated materials gives rise to the transfer of spectral weight from a high to a low energy and the creation of in-gap electronic states [23]. Recently, these in-gap states have been imaged directly by scanning tunneling microscopy in a Mott insulator close to a lattice defect [24]. We have performed LDA + DMFT numerical calculations to obtain the DOS in the presence of weak doping for GaTa_4Se_8 , a member of the GaM_4Q_8 family of Mott insulators used in this study [25]. As shown in Fig. 1(b) and in Fig. S2 [25], the computed DOS in the weak doping

regime presents a gap with an additional peak below the conduction band, which is reminiscent of the localized in-gap states in Fig. 1(a). These strongly correlated states actually have a very heavy effective mass, which diverges in the zero-doping limit [30]. Hence, they may be expected to have low mobility and be prone to localize by lattice imperfections.

The relevance of Fröhlich's model for Mott insulators is further reinforced by recent theoretical calculations performed in the Hubbard-Holstein [31] and in the photodoped dynamic Hubbard models [32]. These studies have pointed out the formation of polaroniclike in-gap states under photodoping or dc-like experiments. Polaronic in-gap states appear instantaneously below the upper Hubbard band when photocarriers are generated in a Mott insulator. These states extend over more than half of the gap width and couple directly to the doublons. Consequently, the creation of the polaronic states induces a rapid thermalization of the doublons generated in the Mott insulator. Therefore, these calculations suggest that, rather remarkably, Mott insulators gather the basic ingredients assumed in Fröhlich's model.

The theory of the dielectric breakdown in the dirty limit is based on the thermal balance of the electronic system, which consists of the energy transfer rates from the electric field to the conduction electrons (gain) and from the electrons localized in shallow levels to the lattice (loss), as shown in Fig. 1(c). Under an electric field, the electronic temperature T_e rises above the lattice-bath temperature T_0 until the two energy transfer rates (gain and loss) equilibrate [see Fig. 1(d)]. More importantly, above a threshold field E_{th} , the energy rates gained and lost by the electrons can no longer be equilibrated. As a consequence of this collective phenomenon, the electronic temperature rises drastically and induces the electrical breakdown [19].

Several measurable predictions are derived from this two-temperature model [19]. First, the temperature dependence of the threshold field is thermally activated such as

$$E_{th} \propto \exp\left(\frac{\Delta\varepsilon}{4kT}\right). \quad (1)$$

Second, the rising of the electronic temperature implies that below the threshold field a nonlinear electrical behavior exists (i.e., a deviation from Ohm's law). The theory predicts that in the low field limit ($E/E_{th} \ll 1$), for which T_e is close to T_0 , the ratio $\sigma(E)/\sigma(E=0)$ becomes temperature independent:

$$\left.\frac{\sigma(E)}{\sigma_0}\right|_{E \ll E_{th}} = \exp\left(\frac{E^2}{E_{th}^2} \frac{\varepsilon_G}{e\Delta\varepsilon}\right) \quad (2)$$

with e Euler's constant.

Moreover, when the field tends to the threshold field ($E/E_{th} \approx 1$), the conductivity ratio tends to the value

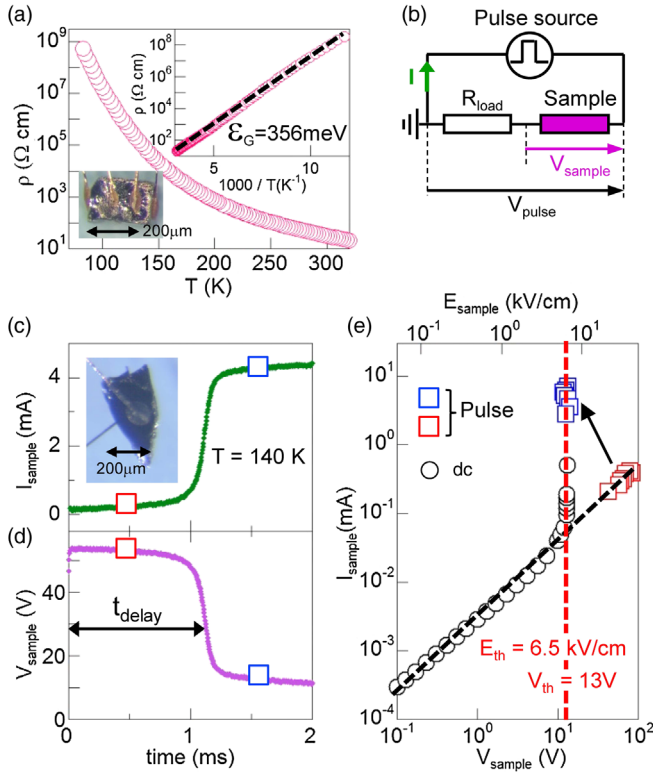


FIG. 2. Resistive transition under electric pulses in the Mott insulator GaMo_4S_8 . (a) Temperature dependence of the resistivity represented as a function of T or $1000/T$ (top inset). The dashed line in the top inset represents the fit by an activated law. The lower inset shows a picture of the sample. (b) Schematic description of the experimental setup. (c),(d) An example of a resistive transition under an electrical field. The inset shows the sample with the electrodes connected on two opposite faces. (e) I - V characteristics of the same sample measured in dc (black circles) or extracted from pulse measurements (c),(d) before and after the resistive transitions (red and blue squares, respectively). The black dotted line gives a linear Ohmic behavior for comparison.

$$\frac{\sigma(E)}{\sigma_0} \Big|_{E \rightarrow E_{\text{th}}} = \exp\left(\frac{\varepsilon_G}{\Delta E}\right). \quad (3)$$

Finally, this kind of breakdown does not occur if the density N_i is too low to interact efficiently with the conduction electrons. This corresponds to the clean limit regime that could occur at a sufficiently low temperature and where an avalanche breakdown could occur by impact ionization. In this regime, the threshold field is expected to increase with the temperature in contrast to the breakdown field in the dirty limit.

The GaM_4Q_8 ($M = \text{V}, \text{Nb}, \text{Ta}, \text{Mo}$; $Q = \text{S}, \text{Se}$) compounds used for this study have been shown to be canonical Mott insulators sharing the same lacunar spinel structure but with narrow gaps depending on their chemistry and ranging from 0.1 to 0.4 eV [33–35]. Figure 2 summarizes the typical response to a dc electric field measured in GaMo_4S_8 , which is analogous to the one observed in other

GaM_4Q_8 compounds [33,36–38]. Figure 2(a) displays the temperature dependence of the resistivity, showing a thermally activated behavior with a gap ε_G of 356 meV. When an electric field pulse exceeding a threshold field E_{th} of a few kV/cm is applied to these compounds, thanks to the circuit sketched in Fig. 2(b), an abrupt drop of the voltage across the sample and an increase of the intensity within the circuit are observed as shown in Figs. 2(c) and 2(d) [33,37,38]. Such transitions called resistive switching occur after a delay t_d in the millisecond range. A series of short electric pulses allows us to draw the current-voltage characteristic of the GaMo_4S_8 sample. This I - V curve is very specific and consists in two branches [see Fig. 2(e)]. The first one corresponds to the nontransited state that deviates slightly from Ohm’s law at a low field as will be discussed in more detail in the following. The second branch, related to the “transited” state, is almost vertical, which means that the sample voltage after the transition always lies on the same value. It also corresponds to the threshold voltage in continuous dc measurements [also shown in Fig. 2(e)].

Figure 3(a) displays the temperature dependence of the threshold field E_{th} obtained for several GaMo_4S_8 single

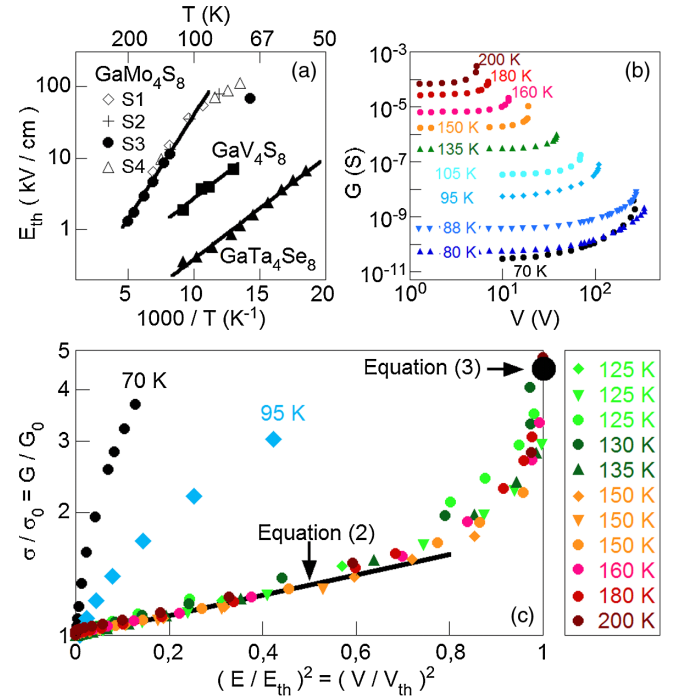


FIG. 3. Electrical response of GaMo_4S_8 , GaV_4S_8 , and GaTa_4Se_8 Mott insulators compared to Fröhlich’s theory. (a) Temperature dependence of the threshold field E_{th} for these three compounds. Four GaMo_4S_8 samples (S1–S4) have been measured. The black lines are fits with Eq. (1). (b) Voltage dependence of the conductance measured below the threshold field in GaMo_4S_8 for several temperatures. (c) Data from (b) displayed as normalized conductance G/G_0 versus squared normalized voltage $(V/V_{\text{th}})^2$. The black line and the black point correspond to the prediction by Eqs. (2) and (3), respectively, with no fitting parameter.

crystals. All samples give similar results with two temperature regimes. The low-temperature regime is characterized by a saturation of E_{th} with a maximum value of 110 kV/cm at 74 K, while at a high temperature (above 125 K) the threshold field decreases exponentially, following Eq. (1) with $\Delta\varepsilon = 230$ meV. The same type of temperature dependence of the threshold field was measured for two other compounds of the AM_4Q_8 family, namely, GaV_4S_8 and GaTa_4Se_8 [see Figs. 3(a) and S3]. For these compounds also, E_{th} exhibits a thermal activation law, and a fit with Eq. (1) shows that $\Delta\varepsilon$ varies from 114 meV in GaV_4S_8 to 112 meV in GaTa_4S_8 . All these experimental observations point to a remarkable agreement with several key predictions of Fröhlich's theory: the existence of a threshold electric field, of two temperature regimes, and of an activated dependence of E_{th} at a high temperature.

Figure 3(b) shows the conductance G measured for several GaMo_4S_8 samples versus the applied voltage at different temperatures ranging from 70 to 200 K. To compare these experimental data with the model's predictions [i.e., Eqs. (2) and (3)], Fig. 3(c) displays $\sigma(E)/\sigma(E=0)$ versus $(E/E_{\text{th}})^2$ for different temperatures. All data above 125 K obtained on several crystals collapse into a single curve, in agreement with the theory. In the low field limit, this experimental master curve shows a very good agreement with the curve calculated from Eq. (2) using the values ε_G and $\Delta\varepsilon$ determined, respectively, from the $\rho(T)$ and $E_{\text{th}}(T)$ curves. Moreover, the ratio $\sigma(E)/\sigma(0)$ for $E \rightarrow E_{\text{th}}$ reaches a value close to that predicted from Eq. (3), i.e., $\sigma(E)/\sigma(0) = 4.7$, indicated as a black dot in Fig. 2(c). This striking agreement with Fröhlich's theory is not restricted to GaMo_4S_8 but convincingly appears also in GaTa_4Se_8 , as shown in Fig. S3 [25].

This agreement of experimental data with the theory is all the more remarkable considering that both Eqs. (2) and (3) have no adjustable parameters. As expected, in the low-temperature regime for which the electrical breakdown is no longer influenced by the presence of localized in-gap states, the experimental data depart strongly from the predictions for the high-temperature regime. This is particularly clear in Fig. 3(c), where obvious deviations from the master curve appear below 125 K.

All these results show that the Mott insulators studied in this work experience under an electric field an enhancement of electronic conductivity because of the multiplication of charge carriers. This destabilization is a collective phenomenon where the in-gap states play a major role. At a high temperature and below the threshold field, the carrier multiplication vanishes with time, and the electronic temperature can be stabilized above that of the lattice. The low field nonlinear behavior described by the Fröhlich model is therefore a homogeneous phenomenon. But when the electronic system is pushed beyond thermal stability, a dielectric breakdown occurs which is much likely inhomogeneous. Indeed defects, which cannot be avoided in real samples, may induce small local variations of the

electric field and trigger the formation of a filamentary path as proposed in Ref. [37].

In the nonequilibrium regime above the threshold field, the resistive transition occurs abruptly in GaMo_4S_8 at a time t_d after the beginning of the electric pulse, which depends on the strength of the field [see Fig. 4(a)]. The transient properties of the dielectric breakdown have been extensively studied for band insulators in the framework of a laser-induced breakdown [39–45]. The time at which the breakdown occurs is usually defined as the time at which the electric field generates enough free carriers to reach the critical plasma density [39–42] where the system acquires metallic properties. A scaling law exists for pulses longer than 10 ps between the fluence breakdown F_{th} (or the threshold electric field E_{th}) and the pulse width (τ_p) such as $F_{\text{th}} \propto E_{\text{th}}^2 \tau_p \propto \sqrt{\tau_p}$ (i.e., $E_{\text{th}}^4 \propto 1/\tau_p$). In our case, this should lead to a threshold field dependence with a time delay of the form $E_{\text{th}}^4 \propto 1/t_d$. As shown in Fig. 4(b), this is precisely the dependence obtained from the results on

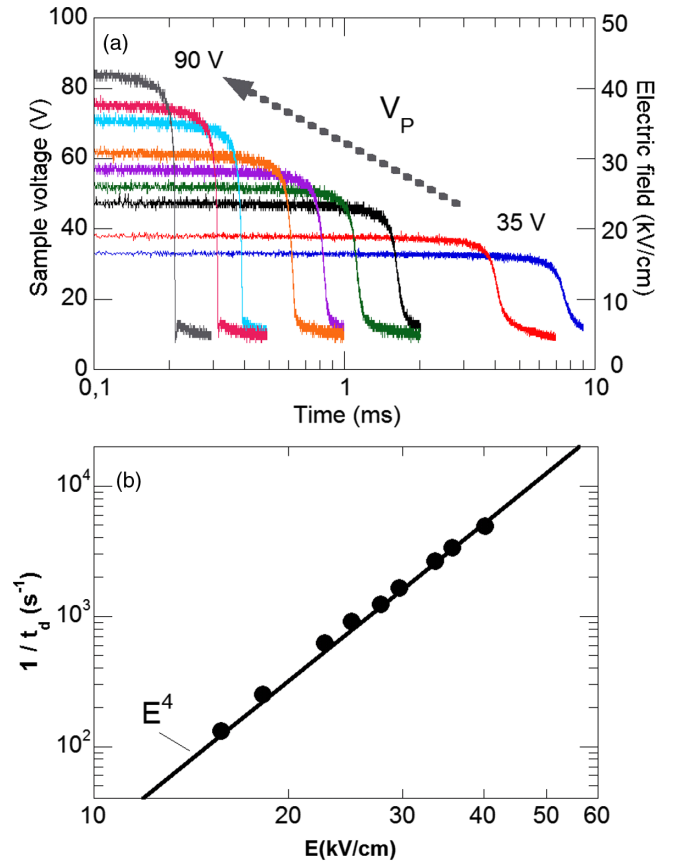


FIG. 4. Dynamics of the dielectric breakdown of GaMo_4S_8 . (a) Time evolution of the sample voltage V_S (left scale) and corresponding electric field (E) in the sample (right scale) during pulses of several amplitudes V_S between 35 and 90 V. The dielectric breakdown starts after a time t_d , which decreases with increasing V_S . (b) Inverse of t_d as a function of the initial electric field through the sample. The black line indicates a quartic field dependence.

GaMo₄S₈, where t_d spreads on 2 orders of magnitude. This very specific dependence of t_d with the electric field appears systematically in all AM_4Q_8 compounds (see Fig. S4 [25]). These results strongly evidence that the resistive transition appears when the electronic system reaches the critical plasma density.

In conclusion, our present results provide a sound microscopic description of the nonlinear transport properties of Mott insulators under electric fields. At a low field, a Mott insulator reaches a steady state with a slight elevation of its electronic temperature above that of the lattice. This steady state is achieved as the power gained by the conducting electrons (thanks to the electric field) is balanced by the power lost by electrons trapped in in-gap states (thanks to electron phonon interactions). This nonlinear electrical behavior was observed in all AM_4Q_8 compounds, and we have shown its remarkable agreement with the Fröhlich theory. Above a threshold electric field, the power gained and lost by electrons cannot equilibrate anymore. In this nonequilibrium regime, the electronic temperature diverges, and when the critical plasma density is reached, the dielectric breakdown occurs. The most prominent signature of this dielectric breakdown is the resistive switching measured in all AM_4Q_8 . Beyond these compounds, the same type of resistive transition was found in the canonical Mott insulators (V, Cr)₂O₃ and Ni(S, Se)₂ [37], which suggests that it should apply for a large variety of correlated materials. Finally, we note that the behavior of Mott insulators under an electric field departs strongly from the one of semiconductors. The electric field generates in Mott insulators a long-lived “hidden” metallic phase characterized by the presence of hot electrons whose control could open the way to new functionalities. A striking example is the leaky integrate and fire functionality recently used to implement a novel type of artificial neuron [46].

This work was supported by the Région Pays de la Loire through the funding of the “pari scientifique Neuro-Mott” and the postdoc fellowship of Pascale Diener. The work was also supported by the ANR project Elastica No. 16-CE30-0018. B. C., E. J., and L. C. thank all participants of the French Japanese International Associated Laboratory “IM-LED Impacting Materials with Light and Electric Fields and Watching Real Time Dynamics” for stimulating discussions dealing with the topic of this article.

The authors declare no competing financial interests.

*Present address: Institute for Electronics Microelectronics and Nanotechnology (IEMN) CNRS, University of Lille BP60069, avenue Poincare, F-59652 cedex, Villeneuve d’Ascq, France.

†Corresponding author.
laurent.cario@cnrs-immn.fr

- [1] K. Nasu, *Photoinduced Phase Transitions* (World Scientific, Singapore, 2004).
- [2] L. Stojchevska, I. Vaskivskiy, T. Mertelj, P. Kusar, D. Svetin, S. Brazovskii, and D. Mihailovic, Ultrafast switching to a stable hidden quantum state in an electronic crystal, *Science* **344**, 177 (2014).
- [3] D. Fausti, R. I. Tobey, N. Dean, S. Kaiser, A. Dienst, M. C. Hoffmann, S. Pyon, T. Takayama, H. Takagi, and A. Cavalleri, Light-induced superconductivity in a stripe-ordered cuprate, *Science* **331**, 189 (2011).
- [4] S. Iwai, M. Ono, A. Maeda, H. Matsuzaki, H. Kishida, H. Okamoto, and Y. Tokura, Ultrafast Optical Switching to a Metallic State by Photoinduced Mott Transition in a Halogen-Bridged Nickel-Chain Compound, *Phys. Rev. Lett.* **91**, 057401 (2003).
- [5] H. Yamakawa, T. Miyamoto, T. Morimoto, T. Terashige, H. Yada, N. Kida, M. Suda, H. M. Yamamoto, R. Kato, K. Miyagawa, K. Kanoda, and H. Okamoto, Mott transition by an impulsive dielectric breakdown, *Nat. Mater.* **16**, 1100 (2017).
- [6] H. Aoki, N. Tsuji, M. Eckstein, M. Kollar, T. Oka, and P. Werner, Nonequilibrium dynamical mean-field theory and its applications, *Rev. Mod. Phys.* **86**, 779 (2014).
- [7] S. Whitehead, *Dielectric Breakdown of Solids* (Clarendon, Oxford, 1951).
- [8] E. Janod, J. Tranchant, B. Corraze, M. Querré, P. Stoliar, M. Rozenberg, T. Cren, D. Roditchev, V. T. Phuoc, M.-P. Besland, and L. Cario, Resistive switching in Mott insulators and correlated systems, *Adv. Funct. Mater.* **25**, 6287 (2015).
- [9] T. Oka, R. Arita, and H. Aoki, Breakdown of a Mott Insulator: A Nonadiabatic Tunneling Mechanism, *Phys. Rev. Lett.* **91**, 066406 (2003).
- [10] S. Okamoto, Nonlinear Transport through Strongly Correlated Two-Terminal Heterostructures: A Dynamical Mean-Field Approach, *Phys. Rev. Lett.* **101**, 116807 (2008).
- [11] F. Heidrich-Meisner, I. González, K. A. Al-Hassanieh, A. E. Feiguin, M. J. Rozenberg, and E. Dagotto, Nonequilibrium electronic transport in a one-dimensional Mott insulator, *Phys. Rev. B* **82**, 205110 (2010).
- [12] M. Eckstein, T. Oka, and P. Werner, Dielectric Breakdown of Mott Insulators in Dynamical Mean-Field Theory, *Phys. Rev. Lett.* **105**, 146404 (2010).
- [13] M. Eckstein and P. Werner, Nonequilibrium dynamical mean-field simulation of inhomogeneous systems, *Phys. Rev. B* **88**, 075135 (2013).
- [14] J. Li, C. Aron, G. Kotliar, and J. E. Han, Electric-Field-Driven Resistive Switching in the Dissipative Hubbard Model, *Phys. Rev. Lett.* **114**, 226403 (2015).
- [15] W.-R. Lee and K. Park, Dielectric breakdown via emergent nonequilibrium steady states of the electric-field-driven Mott insulator, *Phys. Rev. B* **89**, 205126 (2014).
- [16] G. Mazza, A. Amaricci, M. Capone, and M. Fabrizio, Field-Driven Mott Gap Collapse and Resistive Switch in Correlated Insulators, *Phys. Rev. Lett.* **117**, 176401 (2016).
- [17] T. Oka, Nonlinear doublon production in a Mott insulator: Landau-Dykhne method applied to an integrable model, *Phys. Rev. B* **86**, 075148 (2012).

- [18] Y. Taguchi, T. Matsumoto, and Y. Tokura, Dielectric breakdown of one-dimensional Mott insulators Sr_2CuO_3 and SrCuO_2 , *Phys. Rev. B* **62**, 7015 (2000).
- [19] H. Fröhlich, On the theory of dielectric breakdown in solids, *Proc. R. Soc. A* **188**, 521 (1947).
- [20] H. Fröhlich, Theory of electrical breakdown in ionic crystals, *Proc. R. Soc. A* **160**, 230 (1937).
- [21] F. Seitz, On the theory of electron multiplication in crystals, *Phys. Rev.* **76**, 1376 (1949).
- [22] H. Fröhlich and F. Seitz, Notes on the theory of dielectric breakdown in ionic crystals, *Phys. Rev.* **79**, 526 (1950).
- [23] H. Eskes, M. B. J. Meinders, and G. A. Sawatzky, Anomalous Transfer of Spectral Weight in Doped Strongly Correlated Systems, *Phys. Rev. Lett.* **67**, 1035 (1991).
- [24] C. Ye, P. Cai, R. Yu, X. Zhou, W. Ruan, Q. Liu, C. Jin, and Y. Wang, Visualizing the atomic-scale electronic structure of the $\text{Ca}_2\text{CuO}_2\text{Cl}_2$ Mott insulator, *Nat. Commun.* **4**, 1365 (2013).
- [25] See Supplemental Material at <http://link.aps.org/supplemental/10.1103/PhysRevLett.121.016601> for details on the Fröhlich's theory, LDA + DMFT calculations, sample preparation, transport measurements and Figs. S1–S4, which includes Refs. [26–29].
- [26] P. Blaha, K. Schwarz, G. K. H. Madsen, D. Kvasnicka, and J. Luitz, *An Augmented Plane Wave+Local Orbitals Program for Calculating Crystal Properties* (Karlheinz Schwarz, Technische Universität Wien, Austria, 2001).
- [27] D. J. Singh and L. Nordstrom, *Planewaves, Pseudopotentials and the LAPW Method* (Springer, New York, 2006).
- [28] E. Gull, A. J. Millis, A. I. Lichtenstein, A. N. Rubtsov, M. Troyer, and P. Werner, Continuous-time Monte Carlo methods for quantum impurity models, *Rev. Mod. Phys.* **83**, 349 (2011).
- [29] K. Haule, Quantum Monte Carlo impurity solver for cluster dynamical mean-field theory and electronic structure calculations with adjustable cluster base, *Phys. Rev. B* **75**, 155113 (2007).
- [30] G. Georges, W. Kotliar, and K. M. J. Rozenberg, Dynamical mean-field theory of strongly correlated fermion systems and the limit of infinite dimensions, *Rev. Mod. Phys.* **68**, 13 (1996).
- [31] P. Werner and M. Eckstein, Field-induced polaron formation in the Holstein-Hubbard model, *Europhys. Lett.* **109**, 37002 (2015).
- [32] P. Werner and M. Eckstein, Effective doublon and hole temperatures in the photo-doped dynamic Hubbard model, *Struct. Dyn.* **3**, 023603 (2016).
- [33] L. Cario, C. Vaju, B. Corraze, V. Guiot, and E. Janod, Electric-field-induced resistive switching in a family of Mott insulators: Towards a new class of RRAM memories, *Adv. Mater.* **22**, 5193 (2010).
- [34] V. Ta Phuoc, C. Vaju, B. Corraze, R. Sopracase, A. Perucchi, C. Marini, P. Postorino, M. Chligui, S. Lupi, E. Janod, and L. Cario, Optical Conductivity Measurements of GaTa_4Se_8 Under High Pressure: Evidence of a Bandwidth-Controlled Insulator-to-Metal Mott Transition, *Phys. Rev. Lett.* **110**, 037401 (2013).
- [35] A. Camjayi, C. Acha, R. Weht, M. G. Rodríguez, B. Corraze, E. Janod, L. Cario, and M. J. Rozenberg, First-Order Insulator-to-Metal Mott Transition in the Paramagnetic 3D System GaTa_4Se_8 , *Phys. Rev. Lett.* **113**, 086404 (2014).
- [36] V. Guiot, L. Cario, E. Janod, B. Corraze, V. T. Phuoc, M. Rozenberg, P. Stoliar, T. Cren, and D. Roditchev, Avalanche breakdown in $\text{GaTa}_4\text{Se}_{8-x}\text{Te}_x$ narrow-gap Mott insulators, *Nat. Commun.* **4**, 1722 (2013).
- [37] P. Stoliar, L. Cario, E. Janod, B. Corraze, C. Guillot-Deudon, S. Salmon-Bourmand, V. Guiot, J. Tranchant, and M. Rozenberg, Universal electric-field-driven resistive transition in narrow-gap Mott insulators, *Adv. Mater.* **25**, 3222 (2013).
- [38] C. Vaju, L. Cario, B. Corraze, E. Janod, V. Dubost, T. Cren, D. Roditchev, D. Braithwaite, and O. Chauvet, Electric-pulse-driven electronic phase separation, insulator-metal transition, and possible superconductivity in a Mott insulator, *Adv. Mater.* **20**, 2760 (2008).
- [39] J. R. Bettis, Air Force Weapons Laboratory Technical Report No. AFWL-TR-76-61, Kirtland Air Force Base, 1976.
- [40] D. Du, X. Liu, G. Korn, J. Squier, and G. Mourou, Laser-induced breakdown by impact ionization in SiO_2 with pulse widths from 7 ns to 150 fs, *Appl. Phys. Lett.* **64**, 3071 (1994).
- [41] B. C. Stuart, M. D. Feit, S. Herman, A. M. Rubenchik, B. W. Shore, and M. D. Perry, Optical ablation by high-power short-pulse lasers, *J. Opt. Soc. Am. B* **13**, 459 (1996).
- [42] B. C. Stuart, M. D. Feit, A. M. Rubenchik, B. W. Shore, and M. D. Perry, Laser-Induced Damage in Dielectrics with Nanosecond to Subpicosecond Pulses, *Phys. Rev. Lett.* **74**, 2248 (1995).
- [43] E. Yablonovitch and N. Bloembergen, Avalanche Ionization and the Limiting Diameter of Filaments Induced by Light Pulses in Transparent Media, *Phys. Rev. Lett.* **29**, 907 (1972).
- [44] D. W. Fradin, N. Bloembergen, and J. P. Letellier, Dependence of laser-induced breakdown field strength on pulse duration, *Appl. Phys. Lett.* **22**, 635 (1973).
- [45] B. Rethfeld, Free-electron generation in laser-irradiated dielectrics, *Phys. Rev. B* **73**, 035101 (2006).
- [46] P. Stoliar, J. Tranchant, B. Corraze, E. Janod, M.-P. Besland, F. Tesler, M. Rozenberg, and L. Cario, A leaky-integrate-and-fire neuron analog realized with a Mott insulator, *Adv. Funct. Mater.* **27**, 1604740 (2017).